Materials Horizons

Accepted Manuscript

ROYAL SOCIETY OF CHEMISTRY

rsc.li/materials-horizons

Cite this: DOI: 10.1039/c0xx00000x

www.rsc.org/xxxxxx

ARTICLE TYPE

Synthesis of tetranitro-oxacalix[4]arene with oligoheteroacene groups and its nonvolatile ternary memory performance

Pei-Yang Gu,[a,b] Junkuo Gao,[c] Cai-Jian Lu,[a] Wangqiao Chen,[b,d] Chengyuan Wang,[b] Gang Li,[b] Feng Zhou,[a] Qing-Feng Xu,*[a] Jian-Mei Lu*[a] and Qichun Zhang*[b,d]

Received (in XXX, XXX) Xth XXXXXXXXX 20XX, Accepted Xth XXXXXXXXX 20XX
DOI: 10.1039/b000000x

To achieve ultra-high density memory devices with the capacity of 3^n or larger, a novel larger stable oxacalix[4]arene, 4N4OPz, was reported. 4N4OPz exhibited excellent ternary memory behavior with high ON2/ON1/OFF current ratios of $10^{8.7}/10^{4.2}/1$, low switching threshold voltage of -1.80 V/ -2.87 V, and good stability for these three states.

Many applications of organic electronic devices associate with memory devices.[1] The communications between equipments and outside need the devices to send and receive stored information frequently. Thus, it is necessary to develop new materials for fast, non-volatile, inexpensive, reliable, and high-density data storage.[2] Organic memory devices have received a lot of scientific interests not only because of their current remarkable progress but also because of their unique advantages: light weight, printability, and flexibility.[3] Up to now, most of the researches in this field are conducted based on materials with binary storage performance, which do not meet the future storage requirement (ultra-high density: 3^n or larger).[4] Thus, developing ultra-high density memory devices is urgent. Recently, a handful of organic materials with multilevel stable states have already been demonstrated to show an increasing capacity of 3^n or larger.[5] Although "0", "1", and "2" tristable states have been realized in these organic systems, such examples are still rare and it is still highly desirable to develop new organic compounds with a reliable store capacity of 3^n or larger.

Calix[n]arenes have received much attention over last three decades in supramolecular chemistry due to their specific molecular structure, which allows the formation of numerous host-guest complexes.[6] Replacing the bridging carbon atoms with heteroatoms can result in new excellent candidates with intriguing physical and chemical properties. As a matter of fact, oxacalixarenes are an important class of heterocalixarenes by replacing the bridging carbon atoms of calixarenes with oxygen atoms.[7] However, these materials are still in the synthetic stage and their properties remain largely unexplored, especially for organic electronic devices, which might be due to their poor electronic property. In our research, we believe that new Calix[n]arenes with interesting electronic properties could be achieved if catechol groups were replaced by oligoacenes/oligoheteroacenes because they have been widely used as active layers in organic semiconductor devices such as organic field-effect transistors, organic light emitting diodes, organic solar cells or even memory devices.[8,9,10]

In this report, we are interested in larger oxacalix[4]arene with two phenazine groups and four nitro groups because multilevel oxidation states could be stabilized by heteroatoms, and these states are very important to achieve 3^n or larger data storage capacity. Herein, a novel larger oxacalix[4]arene (4,6,25,27-tetranitro-2,8,23,29-tetraoxacalix[4]-36,37-bis(decyloxy)phenazine, abbreviated as **4N4OPz**), which has two different types of electron-withdrawing groups (nitro and pyrazine), has been successfully synthesized and characterized. We believe that **4N4OPz** should have the following advantages: (1) The introduction of O atom could make **4N4OPz** more stable both in ground state and oxidation state; (2) The nitro group has been introduced in electroactive molecules for the applications of memory devices;[11] and (3) The memory device based on **4N4OPz** might exhibit multilevel stable conductivity states in response to the applied voltage because the electron-withdrawing abilities of nitro and pyrazine are different.

The synthetic procedure for **4N4OPz** is depicted in **Scheme 1**. The synthesis of target molecule **4N4OPz** was in two-step steps: First, starting material 1,2-bis(decyloxy)-4,5-diaminobenzene was prepared according to the previous reports.[12] Then, the commercially available 2,5-dihydroxy-1,4-benzoquinone was reacted smoothly with 1,2-bis(decyloxy)-4,5-diaminobenzene in alcohol to afford 7,8-bis(decyloxy)phenazine-2,3-diol in 62 % yield. Second, the as-prepared intermediate was used as the nucleophilic reagent, which condensed with 1,5-difluoro-2,4-dinitrobenzene to produce **4N4OPz** in 12 % yield.

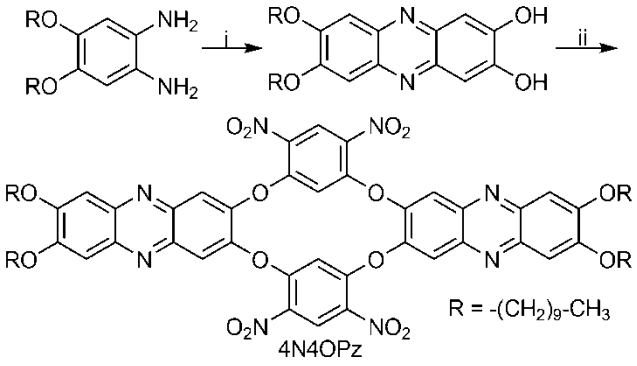

Scheme 1 Synthetic route of compound **4N4OPz**: (i) 1.1 equiv 2,5-dihydroxy-1,4-benzoquinone, CH_3CH_2OH, N_2, reflux, 62 %;

(ii) 1 equiv 1,5-difluoro-2,4-dinitrobenzene, 10 equiv K_2CO_3, DMF, 80 °C, 12 %.

Figure 1a shows the normalized optical absorption and emission spectra of **4N4OPz** in chloroform ($CHCl_3$) and thin film on quartz substrate, respectively. The absorption spectrum of **4N4OPz** exhibits two prominent bands at 276 nm and 434 nm in $CHCl_3$, which can be ascribed to a localized aromatic π-π* transition and intramolecular charge transfer, respectively. **4N4OPz** emits strong green fluorescence with maxima peak at 495 nm (λ_{ex} = 426 nm) in $CHCl_3$ and the fluorescent quantum yield is as high as 13 %. Compared to optical properties of **4N4OPz** in solution, the absorption peaks at both short wavelength and long wavelength are blue-shifted. Note that the absorption edge of **4N4OPz** extends to ~ 478 nm at film state (**Figure S7**), from which the band gap is estimated to be 2.59 eV. Although the emission wavelength of as-prepared film is largely red-shifted (105 nm), the fluorescence density of **4N4OPz** in film is significantly decreased, which might be due to the increasing interactions among molecules in film. These phenomena suggest the H-aggregate formation in film.[13] **4N4OPz** exhibits a very good thermal stability with an onset decomposition temperature of ~ 369 °C (considering the 5% weight loss temperature, **Figure S6**). The excellent thermal property of **4N4OPz** is expected to meet the requirements of heat resistance in the electronics industry.

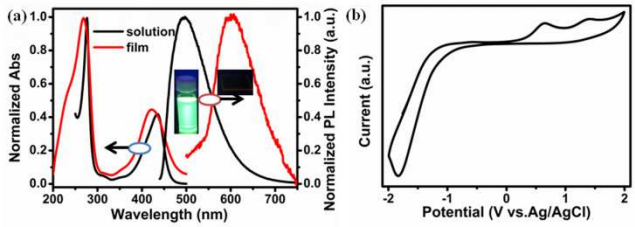

Figure 1 Characterization of **4N4OPz**. (a) Normalized optical absorption and emission spectra of **4N4OPz** in $CHCl_3$ and thin film on a quartz plate, the inset pictures were taken at room temperature under 365 nm UV light. (b) Cyclic voltammograms curve of **4N4OPz** thin films on ITO glass in a 0.1 mol L^{-1} solution of $TBAPF_6$ in acetonitrile solution. The scan rate: 100 mV s^{-1}.

The electrochemical property of **4N4OPz** film on an indium-tin oxide (ITO) glass substrate was studied through cyclic voltammograms (CV) in a 0.1 mol L^{-1} solution of tetrabutylammonium hexafluorophosphate ($TBAPF_6$) in anhydrous acetonitrile solution with a scan rate of 100 mV S^{-1}. As shown in **Figure 1b**, **4N4OPz** exhibits one reduction (-1.84 V) and two oxidation potentials (0.67 and 1.38 V), which correspond to the LUMO, HOMO and HOMO-1 energy levels of ~ -2.56, -5.07 and -5.78 eV using the equation of $E_{LUMO/HOMO} = -e\,(4.40 + E_{red/oxd}^{onset})$ eV.[14] The calculated band gap using CV data is 2.51 eV for **4N4OPz**, which matches very well with the optical onset-edge bandgap result (2.59 eV).

Figure 2a shows the scheme of our prototype memory device, which is similar to the most reported memory devices with a sandwich structure using indium tin oxide (ITO) as bottom electrodes, aluminium (Al, 120 nm thickness) as top electrodes, and an organic layer of **4N4OPz** molecules as an active layer. The **4N4OPz** film thickness was ~ 100 nm, as measured by SEM through a cross section of the film (**Figure 2a**). The atomic force microscopy (AFM) image (Figure **2b**) shows that the film is smooth without aggregation.

The current–voltage (I-V) characteristics of the device were measured by a Hachioji B1500A (Agilent Technologies) semiconductor parameter analyzer. **Figure 2c** shows the typical I-V performances of the as-fabricated device. Starting with the low-conductivity state (OFF, "0"), the current increased slowly with the applied negative voltage sweep. However, a sharp transition from the OFF state to the intermediate-conductivity state (ON1, "1") was observed at switching threshold voltage (STV) of -1.80 V with the increased negative bias. When the negative bias went higher, the current density increased abruptly to 10^{-2} A (ON2, "2") at -2.87 V (sweep 1). These OFF-to-ON1 and ON1-to-ON2 transitions can be regarded as a "writing" process. It remained in the ON2 state when the negative sweep was repeated (sweep 2) or the reverse voltage sweep (sweep 3). These results suggested that once device was switched to ON2 state, the memory device cannot return to both ON1 state and OFF state after turning off the power. Another cell of the device was measured over a voltage range of 0 to -2.5 V (sweep 4) and showed one STV at -1.65 V, indicating the transition from the OFF state to ON1 state. The device remained at ON1 state in the next sweep from 0 to -2.5 V (sweep 5) and 0 to 2.5 V (sweep 6). This result indicated that once the cell reached the ON1 state, this state could be maintained even the power was shut off. In sweep 7 from 0 to -4 V, the storage cell underwent a transition from ON1 state to ON2 state at -2.69 V. Once it was switched to ON2 state, the memory device cannot return to both ON1 state and OFF state (sweep 8-9). The distinctive OFF, ON1, and ON2 states (i.e., different responses to external electric field) can be programmed to correspond to "0", "1", and "2" signals, respectively, suggesting the device's potential application for ternary data storage. It should be worthy of note that the two STVs of our memory device are as low as 3 V, suggesting that the ternary memory device has low-power consumption and is a potential candidate for low-cost and high-performance memory chips in portable nanoelectronic devices. The low STVs of our memory device may be mainly attributed to the formation of H-aggregation, which is favorable for carrier transport. These three states of the ternary memory cell are distinct and the current ratio of "OFF", "ON1", and "ON2" states is 1: $10^{4.2}$: $10^{8.7}$. It is worth noting that the ON2/ON1 and ON1/OFF current ratios in the above device are as high as 10^4, which is enough to promise a low misreading rate through the precise control of the ON2, ON1 and OFF states. This device exhibits a typical write-once read-many-times (WORM) behaviour, which is similar to most of the reported "WORM" devices.[1e,4b] The switching mechanisms could be further confirmed by inserting a LiF thin film as a buffer layer because we believe that holes might dominate the conduction process in ITO/4N4OPz/Al devices and LiF here can be used as a block layer to confirm memory mechanism and performance.[15] As shown in **Figure 2d**, the behaviors of ITO/**4N4OPz**/LiF/Al are similar to those of ITO/**4N4OPz**/Al. In the first sweep from 0 to -4 V, two sharp transitions from the low-conductivity (OFF, "0") state to an intermediate-conductivity (ON1, "1") state, to a high-conductivity (ON2, "2") state were observed at STVs of -1.69 V and -2.61 V, respectively. The three states of the ternary memory cell are also distinct and the current ratio of the "OFF",

"ON1", and "ON2" states is 1: $10^{3.9}$: $10^{8.8}$. To further confirm memory performance, we used metal Pt instead of the Al top electrode. As shown in **Figure S11,** the behaviors of ITO/4N4OPz/Pt are similar to those of ITO/4N4OPz/Al.

Figure 2e/f shows the retention times and stress tests of the memory device for OFF, ON1, and ON2 states. Under a constant stress of -1 V, no significant degradation in current for three different states could be observed for at least 40000 s during the readout test. We also measured the retention times under a constant stress of high voltage or high temperature (50 ^{o}C), there is no significant degradation in current for three different states (**Figure S9**). Moreover, the stimulus effect of continuous read pulses of -1 V on the three different states based on two devices (ITO/4N4OPz/Al and ITO/4N4OPz/LiF/Al) were also investigated. The inset in **Figure S10** shows the pulses (the pulse period and pulse width are 2 us and 1 us) used for the measurements. No current decay was observed after at least 10^7 continuous read cycles. Therefore, the switching behavior on the remnant stored data and the nonvolatile nature of the memory device can explain the functionality of a WORM-type memory characteristic.

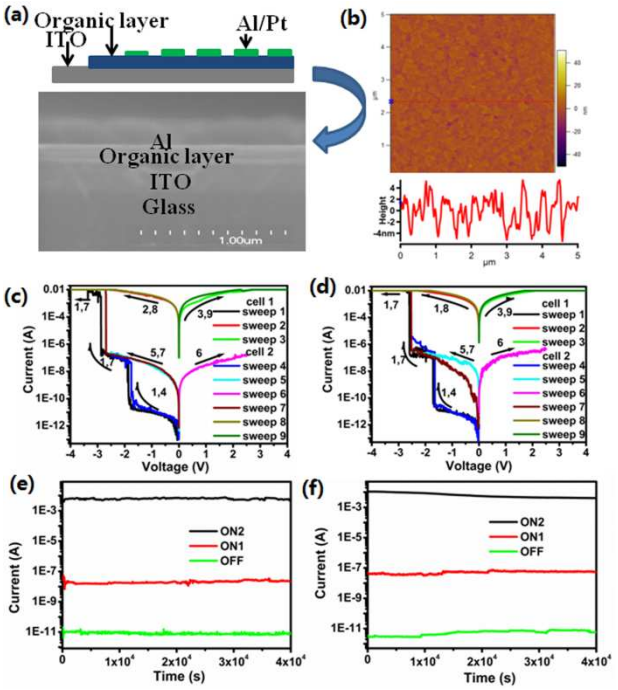

Figure 2 Memory-Device Characteristics of **4N4OPz**. (a) Scheme of the sandwich device and SEM image of a cross section of the device. (b) Tapping-mode (5 μ m × 5 μ m) AFM topography and typical cross-section profile of AFM topographic image of **4N4OPz** film on ITO substrates. (c, d) I-V characteristics of the memory device (ITO/**4N4OPz**/Al and ITO/**4N4OPz**/LiF/Al, respectively) fabricated with **4N4OPz**. (e, f) Stability of the memory device (ITO/**4N4OPz**/Al and ITO/**4N4OPz**/LiF/Al, respectively) in three states under a constant "read" voltage of -1 V at 25 ^{o}C.

To further gain insights into the electronic structure, theoretical calculations were performed using the density functional theory (DFT) method of B3LYP with the 6-31G (d) basis set.[16] **Figure 3a** shows that the HOMO (-6.07 eV) electrons were mainly on the central phenazine units while the LUMO (-2.87 eV) electrons were mainly distributed on tetranitro group, which indicated intramolecular charge transfer from HOMO to LUMO orbits. Thus, the calculated HOMO-LUMO gap was 3.20 eV. From **Figure 3a**, it can be observed that an open channel is formed from the molecular surface throughout the molecule backbone with continuous molecular electrostatic potential (ESP, red), where charge carriers can migrate. However, there are some negative electrostatic potential regions (black) caused by electron-acceptor groups, such as nitro and pyrazine groups. These negative regions can serve as ''traps'' to block the movement of charge carriers. When **4N4OPz** obtained one electron, the HOMO and LUMO orbits were greatly changed. As shown in **Figure 3b**, the electron density distributions of the HOMO (-1.04 eV) mainly locate on tetranitro group while the LUMO (-0.37 eV) orbital is mainly distributed on phenazine group. Moreover, the HOMO-LUMO gap was reduced to 0.67 eV and these negative regions in tetranitro was decreased. When **4N4OPz** obtained two electrons, there were almost no changes in HOMO (1.07 eV) orbit and LUMO (1.27 eV) orbit. The HOMO-LUMO gap was only reduced by 0.20 eV and these negative regions in tetranitro were almost disappeared. If **4N4OPz** obtained more electrons, the HOMO-LUMO gap might be close to 0 eV and these negative regions in pyrazine might be also disappeared. As a result, an open channel is formed from the molecular surface throughout the molecular backbone with continuous molecular ESP, where charge carriers can migrate. To gain insights into the switching mechanisms for the memory devices, energy level diagram for the ITO/**4N4OPz**/Al device is shown in **Figure 4**. The energy barrier (0.27 eV) between the work function of ITO and HOMO of the activer layer is much lower than the energy barrier (1.74 eV) between the work functions of Al and LUMO of the activer layer. Thus, holes might dominate the conduction process in ITO/**4N4OPz**/Al devices. The holes injection barrier is only 0.27 eV, which indicates the low STV. Under low negative voltage, the **4N4OPz** thin film displays a low-conductivity (OFF) state and the current increases slowly because the energy barrier between Al electrode and and LUMO of the activer layer is as large as 1.74 eV, which also blocks the electron migration. Under high bias, holes injection is easier due to the low holes injection barrier (0.27 eV) and the **4N4OPz** has better conductivity at the intermediate-conductivity (ON1) state. At the same time, the HOMO-LUMO gap was reduced and these negative regions in tetranitro were almost disappeared. The lower band gap means the better conductivity. However, two traps are not filled at the same time due to the different ability of accepting electron for nitro and pyrazine groups: the trap of tetranitro is filled and the trap of pyrazine is partly filled, which could be attributed to the stronger ability of accepting electron for tetranitro than that of pyrazine. With the increasing bias, the trap of pyrazine is eventually filled, which leads to the current transition from the ON1 to ON2 state. At the same time, the HOMO-LUMO gap might be reduced to ~ 0 eV. Thus, it is eay to understand the high conductance of the 4N4OPz thin fim at the ON2 state. Consequently, the device shows multilevel memory characteristics due to the two charge traps with different electron-withdrawing ability of tetranitro and pyrazine. The trapped charge carriers were stabilized by intra- and inter- molecular charge transfer forming a charge-separated state and could not be easily de-trapped under reverse bias,

resulting in a high-conductivity state retainable for a long time.

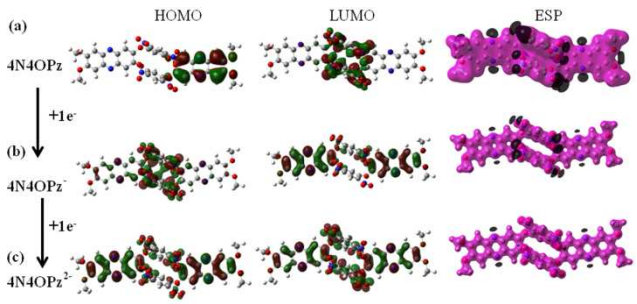

Figure 3 DFT molecular simulation results. (a-c) HOMO and LUMO of **4N4OPz**, **4N4OPz**$^{-}$ and **4N4OPz**$^{2-}$.

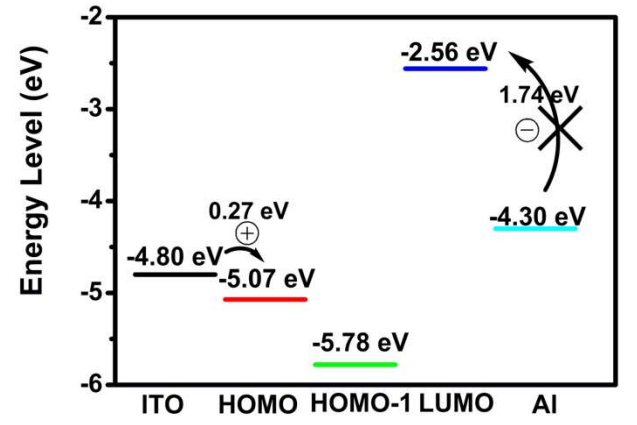

Figure 4 Energy level diagram of HOMO, HOMO-1 and LUMO for 4N4OPz along with the work function of the electrodes.

In summary, we have successfully synthesized a novel larger stable polycyclic aromatic compound, **4N4OPz**, which has two different types of heteroatoms (O and N) and two different types of electron-withdrawing groups (nitro and pyrazine). The sandwich-structure memory devices based on **4N4OPz** exhibited excellent ternary memory behavior with high ON2/ON1/OFF current ratios of $10^{8.7}/10^{4.2}/1$, low switching threshold voltage of -1.80 V/ -2.87 V, and good stability for these three states. The memory performance was confirmed by ITO/**4N4OPz**/LiF/Al and ITO/**4N4OPz**/Pt device. The conduction mechanism through ITO/**4N4OPz**/Al device shows multilevel memory characteristics due to the two charge traps with different electron-withdrawing ability of tetranitro and pyrazine. We believe that our results could provide guidance for the design and synthesis of new heteroacenes, which could be used as promising candidates in nonvolatile memory devices.

Acknowledgements

The authors graciously thank the Chinese Natural Science Foundation (21371128 and 21336005) and Chinese-Singapore Joint Project (2012DFG41900). The work is also supported by the Singapore National Research Foundation through the Competitive Research Programme under Project No. NRF-CRP5-2009-04 (J. G. Y. Z. and C. X.). Q. Z. acknowledges the financial support AcRF Tier 1 (RG 18/09) and Tier 2 (ARC 20/12) from MOE, CREATE program (Nanomaterials for Energy and Water Management) from NRF, and New Initiative Fund from NTU, Singapore.

Notes and references

[a]*College of Chemistry, Chemical Engineering and Materials Science, Collaborative Innovation Center of Suzhou Nano Science and Technology, Soochow University, Suzhou 215123, China. Fax: +86 512 65880367; Tel: +86 512 65880368; E-mail: lujm@suda.edu.cn, xuqingfeng@suda.edu.cn*
[b]*School of Materials Science and Engineering, Nanyang Technological University, Singapore 639798, Singapore. E-mail: qczhang@ntu.edu.sg*
[c]*The Key Laboratory of Advanced Textile Materials and Manufacturing Technology of Ministry of Education, College of Materials and Textiles, Zhejiang Sci-Tech University, Hangzhou 310018, China.*
[d]*Institute for Sports Research, Nanyang Technological University, 50 Nanyang Avenue, Singapore 639798, Singapore*

† Electronic Supplementary Information (ESI) available: [details of characterizations of 4N4OP]. See DOI: 10.1039/b000000x/

1 a) J. Chang, C. Chi, J. Zhang and J. Wu, *Adv. Mater.*, 2013, **25**, 6442; b) Y. Wu, B. Su, L. Jiang and A. J. Heeger, *Adv. Mater.*, 2013, **25**, 6526; c) J.□C. Scott and L.□D. Bozano, *Adv. Mater.*, 2007, **19**, 1452; d) S. Moller, C. Perlov, W. Jackson, C. Taussig and S. R. Forrest, *Nature*, 2003, **426**, 166; e) Q. -D. Ling, D. -J. Liaw, C. Zhu, D. S. -H. Chan, E.-T. Kang and K. -G. Neoh, *Prog. Polym. Sci.*, 2008, **33**, 917; f) T. Kushida, C. Camacho, A. Shuto, S. Irle, M. Muramatsu, T. Katayama, S. Ito, Y. Nagasawa, H. Miyasaka, E. Sakuda, N. Kitamura, Z. Zhou, A. Wakamiya and S. Yamaguchi, *Chem. Sci.*, 2014, **5**, 1296; g) B. Koo, H. Baek and J. Cho, *Chem. Mater.*, 2012, 24, 1091; h) Y. Ko, Y. Kim, H. Baek and J. Cho, *ACS Nano*, 2011, **5**, 9918.

2 a) J. Liu, Z. Yin, X. Cao, F. Zhao, L. Wang, W. Huang, H. Zhang, *Adv. Mater.*, 2013, **25**, 233; b) J. Fang, H. You, J. Chen, J. Lin, and D. Ma, *Inorg. Chem.*, 2006, **45**, 3701; c) F. Zhao, J. Liu, X. Huang, X. Zou, G. Lu, P. Sun, S. Wu, W. Ai, M. Yi, X. Qi, L. Xie, J. Wang, H. Zhang and W. Huang, *ACS Nano*, 2012, **6**, 3027; d) J. Liu, Z. Zeng, X. Cao, G. Lu, L. -H. Wang, Q. -L. Fan, W. Huang and H. Zhang, *Small*, 2012, **8**, 3517.

3 a) G. Liu, Q. -D. Ling, E. Y. H. Teo, C. -X. Zhu, D. S. -H. Chan, K. -G. Neoh and E. -T. Kang, *ACS Nano*, 2009, **3**, 1929; b) C. Simão, M. Mas-Torrent, J. Casado-Montenegro, F. Otón, J. Veciana, C. Rovira, *J. Am. Chem. Soc.*, 2011, **133**, 13256; c) C. Wang, J. Wang, P. Li, J. Gao, S. Y. Tan, W. Xiong, B. Hu, P. S. Lee, Y. Zhao and Q. Zhang, *Chem. Asian J.* , 2014, **9**, 779.

4 a) E. Kapetanakis, A. M. Douvas, D. Velessiotis, E. Makarona, P. Argitis, N. Glezos and P. Normand, *Adv. Mater.*, 2008, **20**, 4568; b) C. W. Chu, J. Ouyang, J. -H. Tseng and Y. Yang, *Adv. Mater.*, 2005, **17**, 1440; c) R. J. Tseng, J. Huang, J. Ouyang, R. B. Kaner and Yang, *Nano Lett.*, 2005, **5**, 1077; d) J. Ouyang, C. -W. Chu, C. R. Szmanda, L. Ma and Y. Yang, *Nat. Mater.*, 2004, **3**, 918; e) L. D. Bozano, B.□W. Kean, M. Beinhoff, K.□R. Carter, P.□M. Rice and J.□C. Scott, *Adv. Funct. Mater.*, 2005, **15**, 1933.

5 a) J. -S. Lee, Y. -M. Kim, J. -H. Kwon, J. S. Sim, H. Shin, B. -H. Sohn and Q. Jia, *Adv. Mater.*, 2011, **23**, 2064; b) S. -J. Liu, P. Wang, Q. Zhao, H. -Y. Yang, J. Wong, H. -B Sun, X. -C. Dong, W. -P. Lin and W. Huang, *Adv. Mater.*, 2012, **24**, 2901; c) C. Ye, Q. Peng, M. Li, J. Luo, Z. Tang, J. Pei, J. Chen, Z. Shuai, L. Jiang and Y. Song, *J. Am. Chem. Soc.*, 2012, **134**, 20053; d) A. J. Kronemeijer, H. B. Akkerman, T.Kudernac, B. J. van Wees, B. L. Feringa, P. W. M. Blom and B. de Boer, *Adv. Mater.*, 2008, **20**, 1467; e) J. Wang and G. D. Stucky, *Adv. Funct. Mater.*, 2004, **14**, 409; f) T. Lee, S. -U. Kim, J. Min and J. -W Choi, *Adv. Mater.*, 2010, **22**, 510; g) P. Y. Gu, F. Zhou, J. Gao, G. Li, C. Wang, Q. F. Xu, Q. Zhang and J. M. Lu, *J. Am. Chem. Soc.*, 2013, **135**, 14086.

6 a) G.W. Orr, L. J. Barbour and J. L. Atwood, *Science*, 1999, **285**, 1049; b) B. H. Hong, J. Y. Lee, C. -W. Lee, J. C. Kim, S. C. Bae and K. S. Kim, *J. Am. Chem. Soc.*, 2001, **123**, 10748; c) M. Touil, M. Elhabiri, M. Lachkar and O. Siri, *Eur. J. Org. Chem.*, 2011, 1914.

7 a) Y. Yang, M. Xue and C. F. Chem, *CrystEngComm*, 2010, **12**, 3502; b) A. Kleyn, T. Jacobs and L. J. Barbour, *CrystEngComm*, 2011, **13**, 3175; c) Y. Visitaec, I. Goldberg and A. Vigalok, *Inorg. Chem.*, 2013, **52**, 6779; d) J. L. Katz, M. B. Feldman and R. R. Conry, *Org. Lett.*, 2005, **7**, 91.

8 a) P. T. Herwig and K. Müllen, *Adv. Mater.*, 1999, **11**, 480; b) G. Giri, E. Verploegen, S. C. B. Mannsfeld, S. Atahan-Evrenk, D. H. Kim, S. Y. Lee, H. A. Becerril, A. Aspuru-Guzik, M. F. Toney and Z. Bao, *Nature*, 2011, **480**, 504; c) A. R. Murphy and J. M. J. Fréchet, *Chem. Rev.*, 2007, **107**, 1066; d) M. M. Payne, S. R. Parkin and J. E. Anthony, *J. Am. Chem. Soc.*, 2005, **127**, 8028; e) H. Qu and C. Chi, *Org. Lett.*, 2010, **12**, 3360; f) J. Xiao, H. M. Duong, Y. Liu, W. Shi, L. Ji, G. Li, S. Li, X. –W. Liu, J. Ma, F. Wudl and Q. Zhang, *Angew. Chem. Int. Ed.*, 2012, **51**, 6094; g) Q. Zhang, Y. Divayana, J. Xiao, Z. Wang, E. R. T. Tiekink, H. M. Doung, H. Zhang, F. Boey, X. W. Sun, and F. Wudl, *Chem. Eur. J.* 2010, **16**, 7422; h) J. Xiao, Y. Divayana, Q. Zhang, H. M. Doung, H. Zhang, F. Boey, X. W. Sun, and F. Wudl, *J. Mater. Chem.* 2010, **20**, 8167; i) J. Xiao, S. Liu, Y. Liu, L. Ji, X. Liu, H. Zhang, X. Sun, and Q. Zhang, *Chem. Asian J.* 2012, **7**, 561; j) J. Xiao, C. D. Malliakas, Y. Liu, F. Zhou, G. Li, H. Su, M. G. Kanatzidis, F. Wudl, and Q. Zhang, *Chem. Asian J.* 2012 **4**, 672.

9) a) Q. Maio, *Synlett* 2012, 326; b) D. Q. Liu, X. M. Xu, Y. R. Su, Z. K. He, J. B. Xu, and Q. Miao, *Angew. Chem. Int. Ed.* 2013, **52**, 6222; c) Q. Miao, T. Q. Nguyen, T. Someya, G. B. Blanchet, and C. Nuckolls, *J. Am. Chem. Soc.* 2003, **125**, 10284; d) Z. X. Liang, Q. Tang, R. X. Mao, D. Q. Liu, J. B. Xu, and Q. Miao, *Adv. Mater*. 2011, **23**, 5514. e) Liang Z. X.; Tang, Q.; Xu, and Q. Miao, *Adv. Mater.* 2011, **23**, 1535; f) Q. Tang, Z. X. Liang, J. Liu, J. B. Xu, and Q. Miao, *Chem. Commun*. 2010, **46**, 2977; g) G. Li, H. M. Duong, Z. Zhang, J. Xiao, L. Liu, Y. Zhao, H. Zhang, F. Huo, S. Li, J. Ma, F. Wudl, and Q. Zhang, *Chem. Comm.* 2012, **48**, 5974; h) Y. Wu, Z. Yin, J. Xiao, Y. Liu, F. Wei, K. J. Tan, C. Kloc, L. Huang, Q. Yan, F. Hu, H. Zhang, and Q. Zhang, *ACS Appl. Mater. Interfaces* 2012, **4**, 1883; i) B. Gao, M. Wang, Y. Cheng, L. Wang, X. Jing, and F. Wang, *J. Am. Chem. Soc.* 2008, **130**, 8297.

10 a) U. H. F. Bunz, J. U. Engelhart, B. D. Linder, and M. Schafforth, *Angew. Chem. Int. Ed.* 2013, **52**, 3810; b) B. D. Lindner, J. U. Engelhart, O. Tverskoy, A. L. Appleton, F. Rominger, A. Peters, H. J. Himmel, and U H. F. Bunz, *Angew. Chem. Int. Ed.* 2011, **50**, 8588; c) U. H. F. Bunz, *Pure Appl. Chem.* 2010, **82**, 953; d) U. H. F. Bunz, *Chem-Eur. J.* 2009, **15**, 6780; e) G. Li, Y. Wu, J. Gao, C. Wang, J. Li, H. Zhang, Y. Zhao, Y. Zhao, and Q. Zhang, *J. Am. Chem. Soc.* 2012, **134**, 20298; f) G. Li, Y. Wu, J. Gao, J. Li, Y. Zhao, and Q. Zhang, *Chem. Asian J.* 2013, **8**, 1574; g) J. Li and Q. Zhang, *Synlett*, 2013, **24**, 686.

11 a) G. Liu , B. Zhang , Y. Chen , C. X. Zhu , L. Zeng , D. S. H. Chan , K. G. Neoh , J. Chen and E. T. Kang, *J. Mater. Chem.*, 2011, **21**, 6027; b) X. D. Zhuang , Y. Chen , G. Liu , B. Zhang , K. G. Neoh , E. T. Kang, C. X. Zhu , Y. X. Li and L. J. Niu, *Adv. Funct. Mater.*, 2010, **20**, 2916 .

12. a) C. W. Ong, S. -C. Liao, T. H. Chang and H. -F. Hsu, *J. Org. Chem.*, 2004, **69**, 3181; b) S. V. Bhosale, C. Jani, C. H. Lalander and S. J. Langford, *Chem. Commun.*, 2010, **46**, 973-975.

13 a) A. D. Hendsbee, C. M. Macaulay and G. C. Welch, *Dyes and Pigments*, 2014, **102**, 204; b) T. K. An, S. –H. Hahn, S. Nam, H. Cha, Y. Rho, D. S. Chung, M. Ree, M. S. Kang, S. –K. Kwon, Y. –H. Kim and C. E. Park, *Dyes and Pigments*, 2013, **96**, 756; c) Y. Wang, D. Liu, S. Ikeda, R. Kumashiro, R. Nouch, Y. Xu, H. Shang, Y. Ma and K. Tanigaki, *Appl. Phys. Lett.*, 2010, **97**, 033305.

14 W. Zhang, X. Sun, P. Xia, J. Huang, G. Yu, M. S. Wong, Y. Liu and D. Zhu, *Org. Lett.*, 2012, **14**, 4382.

15 a) S. Wang, P. K. L. Chan, C. W. Leung and X. Zhao, *RSC Advances* 2012, **2**, 9100; b) T. –L. Choi, K. –H. Lee, W. –J. Joo, S. Lee, T. –W. Lee and M. Y. Chae, *J. Am. Chem. Soc.*, 2007, **129**, 9842.

16 a) P. -Y. Gu, C. -J. Lu, Z. -J. Hu, N. -J. Li, T. -T. Zhao, Q. -F. Xu, Q. -H. Xu, J. -D. Zhang and J. -M. Lu, *J. Mater. Chem. C*, 2013, **1**, 2599; b) S. Kim, Q. D. Zheng, G. S. He, D. J. Bharali, H. E. Pudavar,A. Baev and P. N. Prasad, *Adv. Funct. Mater.*, 2006, **16**, 2317.

Graphic Abstract

Synthesis of tetranitro-oxacalix[4]arene with oligoheteroacene groups and its nonvolatile ternary memory performance

Pei-Yang Gu, Junkuo Gao, Cai-Jian Lu, Chengyuan Wang, Gang Li, Feng Zhou, Qing-Feng Xu, Jian-Mei Lu and Qichun Zhang

The memory devices based on 4N4OPz exhibits excellent ternary memory behavior with high ON2/ON1/OFF current ratios and low switching threshold voltage.